Quantifying Mixing Efficiency and Turbulence Properties in a Coaxial Jet using COMSOL

Mohamed El Amine Fodil*, Hocine Mebarek, Mokhtar Bourdim,
Maghnia University Centre, Tlemcen– Algeria.

Abstract

This paper investigates the mixing and turbulence characteristics of a 2D axisymmetric air/air coaxial jet using COMSOL Multiphysics. The coaxial jet under study consists of a central jet with a diameter of 0.26 cm and a velocity of 12 m/s, surrounded by a co-flowing jet with a diameter of 0.58 cm, whose velocity is defined by the ratio Uco=Ru. Uj is the velocity ratio of the two jets.

The study explores the influence of different parameters, including the velocity ratio, diameter ratio, and Reynolds number, on the flow characteristics. Numerical simulations performed with COMSOL allow for analyzing the velocity and pressure distributions, turbulent kinetic energy, turbulent dissipation rate, and vorticity.

By comparing the results obtained with previous studies, this research aims to deepen the understanding of mixing and turbulence mechanisms in coaxial jets. The study's findings will contribute to identifying optimization strategies to enhance the performance of jet systems and serve as a basis for future research, particularly in exploring the effects of combustion and density variations on jet flows.

Keywords : COMSOL, turbulent jets, k-epsilon, vorticity.

1. Introduction

Coaxial jets consist of a central jet and a co-flowing jet that surround the central jet. Coaxial jets is a complicated flow system that has important applications in various fields, including combustion and propulsion systems. The interactions between the two jets can produce very complex dynamics that affect the velocity distribution, turbulent kinetic energy, turbulent dissipation rate, and vorticity, which are important parameters for optimizing the performance of jet systems.

There has been an extensive body of research in recent years to understand the phenomenology of coaxial jets; thermal effects, swing of density, mixing, turbulence etc., be it numerically or experimentally. In particular, research reported by Afroz and Sharif (2021), Bennewitz et al. (2021), Larsson et al. (2020), Hofmann et al. (2007), Zhang et al. (2022,2023) and Pei et al. (2024) have gone a long way to elucidate the complexities of coaxial jet flows and their effects on numerous industrial practices. In addition, several numerical studies on thermal jets, notably Fodil et al. (2018,

2022), have recognized the salient role of variation in density and the entropy generation factor to the understanding of jet dynamics.

This study falls under this avenue of study and seeks to add to the understanding of mixing and turbulence mechanisms in coaxial jets. Using advanced numerical modeling tools like COMSOL, we will study the distributions of velocity, turbulent kinetic energy, turbulent dissipation rate, and vorticity in order to derive strategies to optimize jet systems. The results will be compared to experimental data from Djiridane (1994).

With this study, we are looking to achieve two important outcomes: we are going to offer optimization approach to improve jet system performance and provide a platform for future study of coaxial jets, especially in relation to combustion effects and density changes in jet flows.

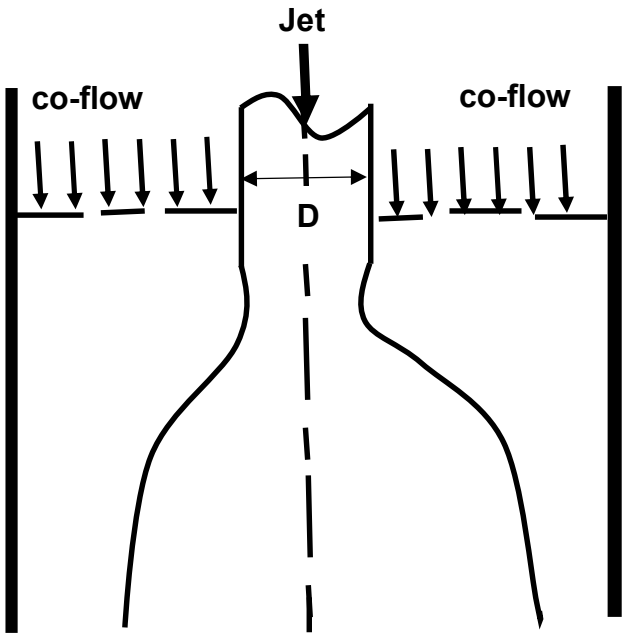

Figure 1 : Schematic of the co-flowing air jet

Case	*Tj (°K)*	*ρo kg/m3*	*Uj m/s*	*Dj mm*	*Ua m/s*	*Re*
1 : Ru = 0.1	290	1.21	12	2.6	1.2	645
2 : Ru = 1	290	1.21	12	2.6	12	6453
3 : Ru = 5	290	1.21	12	2.6	60	32267
4 : Ru = 10	290	1.21	12	2.6	120	64533
5 : Ru = 15	290	1.21	12	2.6	180	96800
6 : Ru = 25	290	1.21	12	2.6	300	161333

Table 1. Characteristics of the studied cases

2. Simplifying assumptions

- The fluid used is assumed to be Newtonian, isotropic and homogeneous.
- The flow is two-dimensional and incompressible.
- The regime is turbulent and permanent.
- Heat transfer and radiation are neglected.

3. Continuity equation

It is the mass conservation equation that expresses the fact that in any flow mass is conserved. The conservative form of the partial differential equation is:

$$\frac{\partial \rho}{\partial t} + div(\rho.\vec{v}) = 0 \qquad (1)$$

If we consider a constant velocity field in space, and for an incompressible fluid, equation **(3)** reduces to the following form:

$$\frac{\partial u}{\partial x} + \frac{\partial v}{\partial y} = 0 \qquad (3)$$

4. Conservation equation of momentum

This equation is obtained by applying the fundamental law of dynamics to a particle of the continuous medium. The forces to be considered are of two types: the volume forces and the surface forces. The equation of motion is written as:

$$\rho \frac{\partial \vec{v}}{\partial t} + \rho(\vec{v}.\nabla)\vec{v} = div\left(\overline{\overline{\sigma}}\right) + \rho\vec{g} \qquad (4)$$

With $\overline{\overline{\sigma}}$ indicate the tensor of the stresses. By neglecting the viscous stresses, one obtains:

$$\rho \frac{\partial \vec{v}}{\partial t} + \rho\left(\vec{v}.\nabla\right)\vec{v} = -\nabla P + \rho\vec{g} \qquad (5)$$

By using the basic notions of scalar products, defining the constraints involved and assuming the volume forces are (buoyancy effects), equation **(3)** can be written in the scalar form by the following equations:

According to (Ox):

$$u\frac{\partial u}{\partial x} + \nu\frac{\partial u}{\partial y} = -\frac{1}{\rho_{nf}}\frac{\partial P}{\partial x} + \frac{\mu_{eff}}{\rho_{nf}}\left(\frac{\partial^2 u}{\partial x^2} + \frac{\partial^2 u}{\partial y^2}\right) \qquad (6)$$

According to (Oy):

$$u\frac{\partial u}{\partial x}+v\frac{\partial u}{\partial y}=-\frac{1}{\rho}\frac{\partial P}{\partial y}+\frac{\mu_{eff}}{\rho}\left(\frac{\partial^2 v}{\partial x^2}+\frac{\partial^2 v}{\partial y^2}\right)+\rho g \quad (7)$$

μ_{eff} is the effective viscosity.

ρ is the density of the fluid.

β is the coefficient of expansion.

ρg are the volume forces.

5. Turbulence equation (k-ε model)

It is given by the following relation:

$$\left(\frac{\partial \rho u K}{\partial x}+\frac{\partial \rho v K}{\partial y}\right)=\frac{\partial}{\partial x}\left[\Gamma k\frac{\partial k}{\partial x}\right]+\frac{\partial}{\partial y}\left[\Gamma k\frac{\partial k}{\partial y}\right]+G_K-\varepsilon\rho \quad (8)$$

$\left(\frac{\partial \rho u K}{\partial x}+\frac{\partial \rho v K}{\partial y}\right)$ Represents the rate of change of kinetic energy K

$\frac{\partial}{\partial x}\left[\Gamma k\frac{\partial k}{\partial x}\right]+\frac{\partial}{\partial y}\left[\Gamma k\frac{\partial k}{\partial y}\right]$ Represents the transport by diffusion of kinetic energy.

G_K Represents the production of turbulent kinetic energy by shear.

$\varepsilon\rho$ Represents the dissipation of turbulent kinetic energy K.

Or $\Gamma k=\left(\mu+\frac{\mu_t}{\mu_\varepsilon}\right)$ the production of turbulent kinetic energy by shear.

μ_t is the turbulent viscosity given by $\mu_t=C_\mu\frac{\rho K^2}{\varepsilon}$

$$G_K=3\mu_t\left[\left(\frac{\partial u}{\partial x}\right)^2+\left(\frac{\partial v}{\partial x}\right)^2\right]+\left[\frac{\partial u}{\partial x}+\frac{\partial v}{\partial y}\right]^2 \quad (9)$$

7. Equation of the turbulent kinetic energy dissipation rate

$$\left(\frac{\partial \rho\varepsilon u}{\partial x}+\frac{\partial \rho v\varepsilon}{\partial y}\right)=\frac{\partial}{\partial x}\left[\Gamma\varepsilon\frac{\partial \varepsilon}{\partial x}\right]+\frac{\partial}{\partial y}\left[\Gamma\varepsilon\frac{\partial \varepsilon}{\partial y}\right]+\frac{\varepsilon}{K}C_{\varepsilon 1}G_K-C_{\varepsilon 1}\rho\frac{\varepsilon^2}{K} \quad (14)$$

$\left(\frac{\partial \rho \varepsilon u}{\partial x}+\frac{\partial \rho v \varepsilon}{\partial y}\right)$ Represents the rate of change of ε

$\frac{\partial}{\partial x}\left[\Gamma \varepsilon \frac{\partial \varepsilon}{\partial x}\right]+\frac{\partial}{\partial y}\left[\Gamma \varepsilon \frac{\partial \varepsilon}{\partial y}\right]$ Represents the diffusion transport of kinetic energy dissipation.

$\frac{\varepsilon}{K} C_{\varepsilon 1} G_K$ Represents the rate of production of ε.

$C_{\varepsilon 1} \rho \frac{\varepsilon^2}{K}$ Represents the dissipation ε.

Or: $\Gamma_\varepsilon = \left(\mu + \frac{\mu_t}{\mu_\varepsilon}\right)$

μ_t is the turbulent viscosity given by $\mu_t = C_\mu \frac{\rho K^2}{\varepsilon}$

Production of turbulent kinetic energy:

$$G_K = 3\mu_t \left[\left(\frac{\partial u}{\partial x}\right)^2 + \left(\frac{\partial v}{\partial x}\right)^2\right] + \left[\frac{\partial u}{\partial x} + \frac{\partial v}{\partial y}\right]^2 \quad (10)$$

The coefficients of the K-standard model are grouped together in **Table 2**.

$C\mu$	C_{e_1}	C_{e_2}	σ_k	σ_ε	K_V	B
0.09	1.44	1.92	1.0	1.3	0.41	5.2

Table 2. Constants of turbulence model.

8. **Numerical method**

A numerical simulation of the coaxial jet was conducted using COMSOL Multiphysics, a finite-element simulation software. The numerical model utilizes the steady-state Navier-Stokes equations with a structured mesh in a 2D computational domain. The jet was simulated as an axisymmetric turbulent jet; the velocity ratio (Ru) is defined by Ru = Uco/Uj, where Uj = 12 m/s and Ru ranges from 0.1 to 25 (as presented in Table 1). The turbulence closure used for the Navier-Stokes equations is the standard two-equation K-ε model.

This approach will enable the study of the effects of different parameters on the flow characteristics, notably the velocity ratio of the two jets, the diameter ratio of the two jets and the Reynolds number. The analysis will be conducted upon the distribution of velocity and pressure, turbulent kinetic energy, turbulent dissipation rate and vorticity. The results obtained will be compared to the results obtained experimentally by Djiridane (1994).

9. Results and Discussion

9.1 Axial Evolution of Mean Velocity for Ru=0.1

The timeline shows the steady drop in average velocity versus normalized distance x/D (where D is the jet diameter). For Ru=0.1, the co-flowing jet velocity (Uco) is small relative to the central jet velocity, and this results in a significant velocity gradient and rapid initial mixing. While the velocity gradient diminishes as axial distance increases, the mean velocity diminishes as a direct result of the momentum transfer between the central and co-flowing jets.

Maximum and Minimum Positions:

At the outlet (near x/D=0), the mean velocity is at a maximum, which is where the initial kinetic energy injection is at its strongest. As we move further from the outlet, the velocity decreases gradually towards minimum values at large distances (large x/D) where the effect of the central jet is practically negligible and mixing has occurred.

Numerical and Experimental Comparison:

The diamonds in the curve represent the experimental data for Djiridane (1994), and the black curve presents the numerical findings conducted for Uco=1.2 m/s. There is a good agreement in numerical and experimental data, particularly in the area where the velocity begins to decline. The discrepancy between the two curves can be attributed to experimental uncertainty and the assumptions of the numerical model.

The figure illustrates the numerical model's capacity to represent the overall behaviour of the time-averaged receding mean velocity in a coaxial jet. The findings demonstrate that the numerical model is valid because of the agreement with the experimental data for Djiridane (1994) and aim to explore the complexity of the mixing phenomenon between the central and the co-flowing jets.

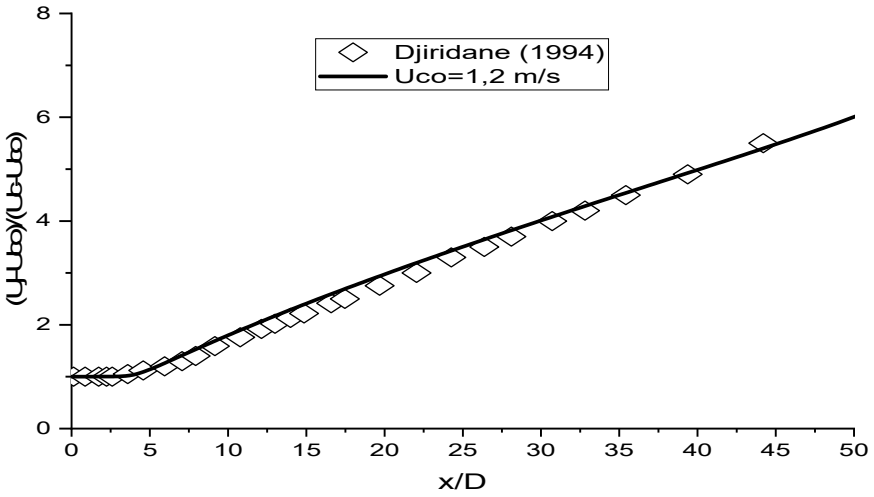

Figure 2 : Mean velocity profile along the axial direction

9.2 Axial Evolution of Turbulent Kinetic Energy for Different Ru Values

Turbulent kinetic energy, which is connected to fluctuations in velocity, reaches its maximum and minimum values at the locations of the maximum and minimum velocity gradients, respectively. For low Ru values (for instance Ru=0.1), the turbulence kinetic energy is high because the velocity within the turbulence layer fluctuates greatly between the fast jet flow and the slow co-flowing jet near the outlet. Although, as the Ru increases, the turbulence kinetic energy generally decreases since lower initial velocity gradient means lower turbulence levels.

Maximum and Minimum Positions :

The location of maximum kinetic energy is typically around the jet outlet, between approximately x/D=1 and x/D=3, where the velocity gradient is largest and turbulence develops quickly. The location of minimum kinetic energy is further downstream, at increasing x/D positions beyond where mixing and diffusion of the velocities have reduced velocity fluctuations. The low values of turbulent kinetic energy downstream from the sustained jet portion of flow result from the loss of shear force at the merging jets, which causes the flow to become more uniform.

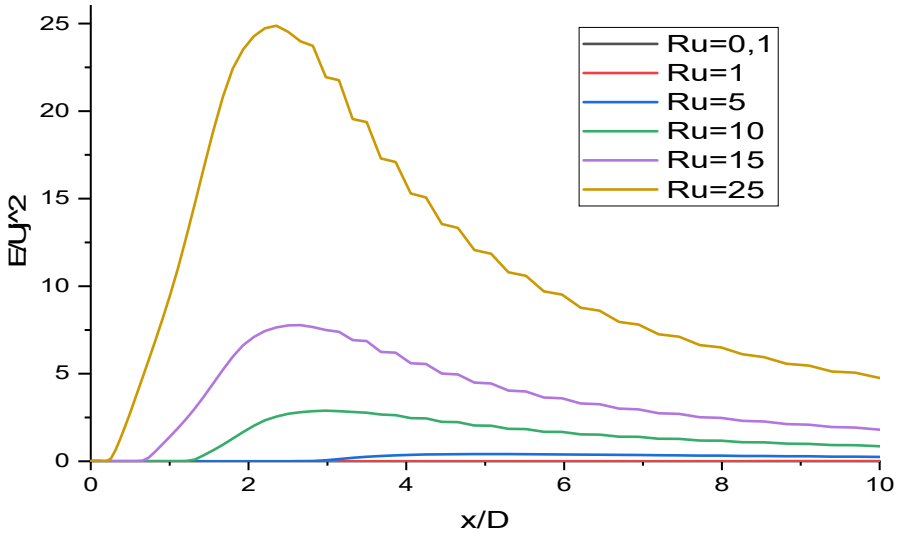

Figure 3: Mean Turbulent Kinetic Energy profile along the axial direction

9.3 Axial Evolution of Turbulent Dissipation Rate for Different Ru Values

The turbulent dissipation rate is a measure of the conversion of turbulent kinetic energy into heat through viscous effects and is typically proportional to the small scales of turbulence. The turbulent dissipation rate is high near the jet exit when Ru is low because fluctuations and velocity gradients are large. As Ru increases, a smaller initial velocity gradient leads to less turbulence in general, and thus a lower turbulent dissipation rate.

Maximum and Minimum Positions :

The highest levels of dissipation occur near the outlet. In the first x/D=1 to x/D=3, the velocity gradients are high, and turbulence dissipates quickly as a result of the strong interaction between the central jet and the co-flowing jet. Overall, this yields an average dissipation rate contribution that trends quickly towards zero and no longer acts as a case for breakup. Minimum levels of dissipation occur further downstream towards large values of x/D, where turbulence has been largely dissipated, and the flow is stabilized and has a homogeneous flow structure with minimal velocity fluctuations.

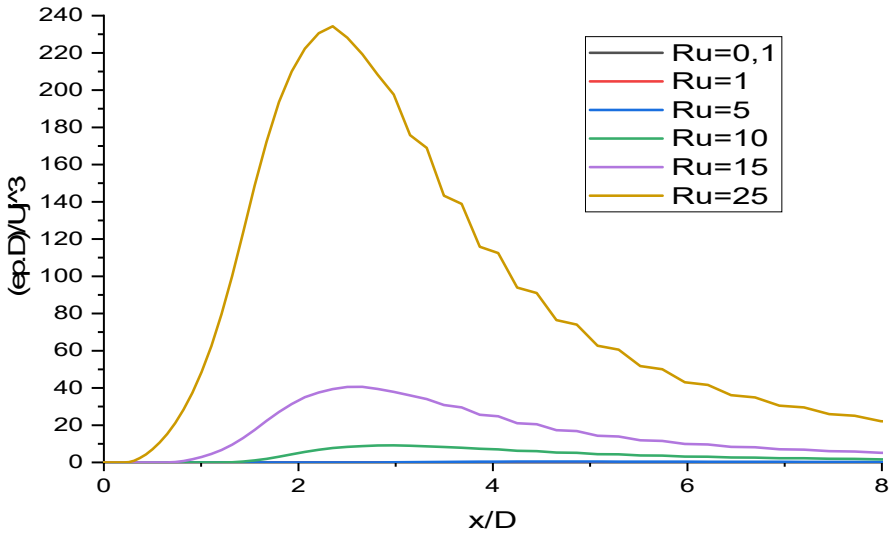

Figure 4: Mean Turbulent Dissipation Rate profile along the axial direction

9.4 Axial Evolution of Vorticity for Different Ru Values

Vorticity, which signifies the local rate of rotation of fluid particles, is greatly affected by the velocity gradients of the central jet and the co-flow. At low Ru, the significant shear of the two jets produces higher vorticity values near the outlet. By increasing Ru, the velocities of the two jets are closer to each other, which reduces the velocity gradients and vorticity.

Maximum and Minimum Positions :

The region near the outlet (between x/D=1 and x/D=2) is where the maximum vorticity occurs because there are the highest velocity gradients. Sharp initial differences in the velocities of the two jets will lead to large amounts of shear, which results in increased rotation of the fluid and increased vorticity.

The minimum vorticity occurs at a large distance in the axial direction, toward larger values of x/D, where the mixing of the two jets is complete due to the smaller differences in velocity, decreasing shear, and leaving the fluid with very little rotation.

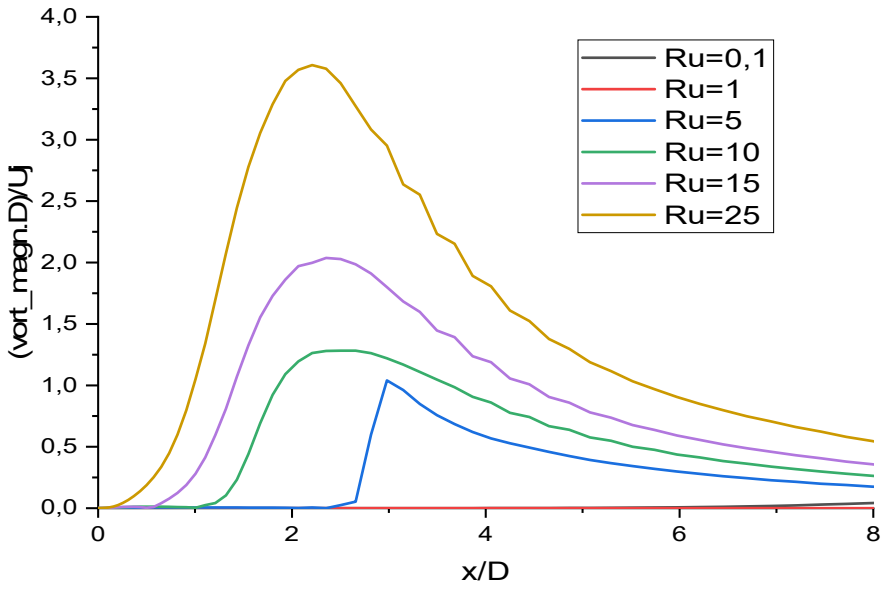

Figure 5: Mean Vorticity profile along the axial direction

9.5 velocity contours and streamlines for Different Ru Values (Ru=5, Ru=10, Ru=15, Ru=25)

The velocity contours and streamlines contour maps provide insights into the velocity distribution in the flow field as a function of Ru. For lower Ru, the velocity at the center is concentrated with contours closely clustered along the jet axis, indicating a strong velocity gradient. As Ru is increased, the velocity distribution spreads axially; contours begin to approach a more homogeneous distribution, and the velocity field is becoming more uniform. This change is a result of the decreasing differences in velocity between the two jets; as differences become smaller, the flow field is stabilizing and losing its turbulent nature.

In general, the position of maximum and minimum kinetic energy, dissipation rate, and vorticity are a direct result of velocity gradients and distance from the outlet. When close to the outlet (x/D=1), maxima are typically found because of strong initial interactions between the jets. As the jets move downstream and mixing occurs along with velocity gradients declining, the values of these variables also are diminished, leading to a more stable homogeneous flow.

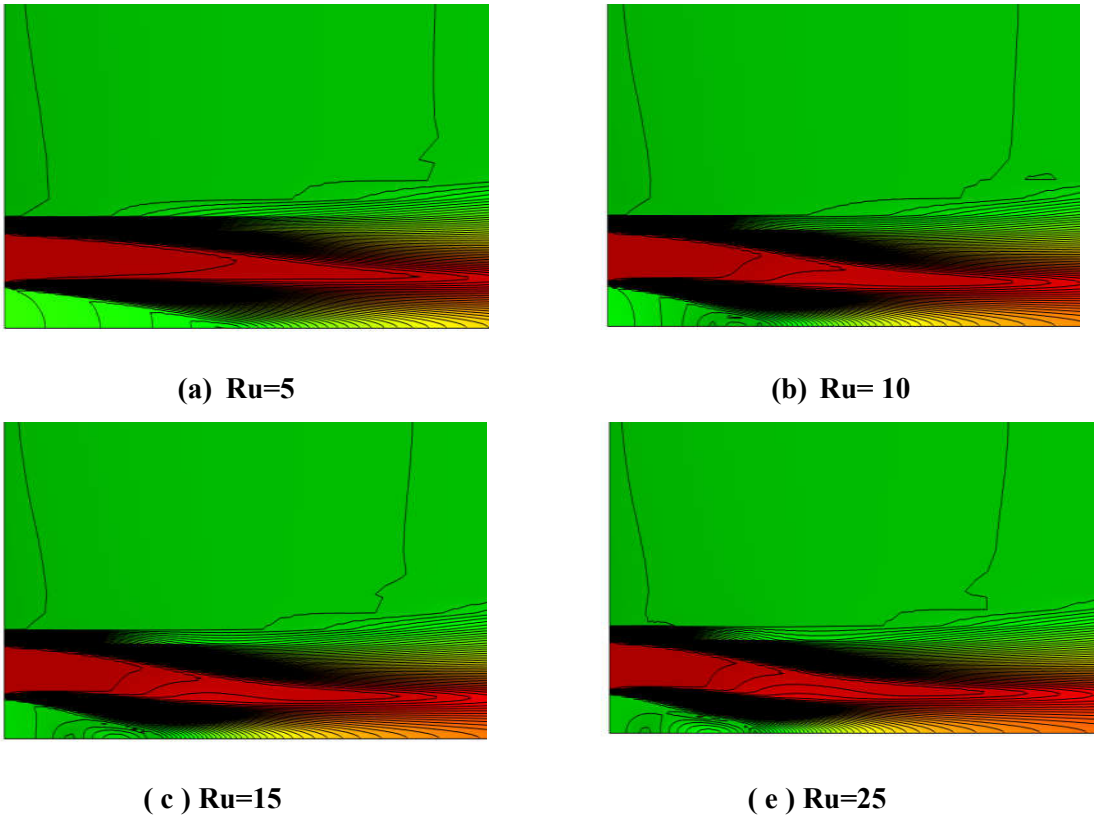

(a) Ru=5 **(b) Ru= 10**

(c) Ru=15 **(e) Ru=25**

Figure 6: Axial velocity contours and streamlines for different velocity ratios

Conclusion

Using COMSOL Multiphysics, the study of mixing and turbulence features of a coaxial jet provided insights into a number of significant features of jet flow. Utilizing a 2D axis symmetric air/air model with a center jet of 0.26 cm and velocity of 12 m/s co-flowing jet with diameter 0.58 cm and velocity defined by the ratio Uco = Ru·Uj. The model allowed us to analyze the influence of a number of parameters on jet flow features.

The simulations indicated that velocity ratio of the two jets, diameter ratio of the two jets, and Reynolds number were all governing factors in the velocity distribution, pressure distribution, turbulent kinetic energy, turbulent dissipation rate, and vorticity. The results indicate that increasing Reynolds number resulted in increased turbulence and vorticity which both have direct effects on liquid mixing. Additionally, changing the velocity and diameter ratios of the jets influenced the velocity and pressure profiles impacting system performance.

We compared our results with published data to validate our simulations, and identify similar trends and varying dynamics of coaxial jets. Fodil et al.'s (2022) work on thermal jets with entropy generation and Larsson et al.'s research (2020) on turbulent coaxial jets provided useful benchmarks for our analysis. Similar numerical simulations enhanced the process of analyzing mixing and

turbulence mechanisms to characterize coaxial jets, consistent with Ba et al. (2023) and Ivanic (2002) who made observations to examine vigorous mixing processes.

Nomenclature		
D	Jet diameter	**[m]**
k	Turbulence kinetic energy	**[m²/s²]**
K_u	Axial decrease rate	**[1]**
Ru	Injection rate, Ua / Uj	**[1]**
P	Pressure.	**[Pa**
Re	Reynolds number.	**[1]**
R_ρ	Densities ratio = ρ_a / ρ_j	**[1]**
U	velocity	**[m/s]**
G_K	Turbulent shear kinetic energy	**[m²/s²]**
$X_{k\max}$	limit of the potential core	**[1]**
L	Length	**[m]**
D	Diameter	**[m]**

Greek symbols		
β	Spatial dilatation coefficient.	**1/K**
ε	Dissipation rate of the k energy	**[m²/s³]**
μ	Dynamicviscosity	**[Pa.s]**
υ	Viscosity	**[m²/s]**
ρ	Density	**[kg/m³]**
α	Thermal diffusion	**[m²/s]**
λ	Thermal conduction coefficient	**[W/(m·K)]**
σ	Stefan -Boltzmann constant	**[W/(m²·K⁴)]**

Indices et exposants		
t	Turbuent	/
f	*Flow*	/
j	Jet	/
a	Co-flow	/

Acknowledgment

We would like to thank the Institute of science and technology of the University centre of Maghnia Algeria for their support during the realization of this work.

Reference

1. Fodil, M.A., Meftah, S.M., and Imine, B. (2018). Numerical study of non-reactive confined thermal jet with variable density. Computational Thermal Sciences, Vol (10), pp. 297-305.
2. Fodil, M.A., and al. (2022). Use of COMSOL in Numerical Study of Thermal Jet with Entropy Generation. Computational Thermal Sciences, Vol (14), pp. 19-30
3. Afroz, F., & Sharif, M.A.R. (2021). Heat Transfer from a Heated Flat Surface Due to Swirling Coaxial Turbulent Jet Impingement. J. Thermal Sci. Eng. Appl., 13(2), 021009.
4. Bennewitz, J.W., Schumaker, S.A., Lietz, C.F., & Kastengren, A.L. (2021). Scaling of oxygen-methane reacting coaxial jets using x-ray fluorescence to measure mixture fraction. Proceedings of the Combustion Institute, 38(4), 6365-6374.
5. Larsson, I. A. S., Lycksam, H., Lundström, T. S., & Marjavaara, B. D. (2020). Experimental study of confined coaxial jets in a non-axisymmetric co-flow. *Experiments in Fluids*, *61*(256).
6. Hofmann, H. M., Movileanu, D. L., Kind, M., & Martin, H. (2007). Influence of a pulsation on heat transfer and flow structure in submerged impinging jets. *International Journal of Heat and Mass Transfer*, *50*(17-18), 3638-3648.
7. Ivanic, T. (2002). *Etude des instabilités générées par deux jets tournants coaxiaux* [Doctoral thesis, Université de Poitiers]. École doctorale Sciences pour l'ingénieur et aéronautique.
8. Janetzke, T., & Nitsche, W. (2009). Time resolved investigations on flow field and quasi wall shear stress of an impingement configuration with pulsating jets by means of high-speed PIV and a surface hot wire array. *International Journal of Heat and Fluid Flow*, *30*(5), 877-885.
9. Zhang, B., Usta, M., Khan, I., Ranjan, D., & Aidun, C. K. (2023). Chemically reacting mixing in coaxial miscible liquid jets under variable viscosities and reaction rates. *Chemical Engineering Science*, *268*, 118412.

10. Zhang, B., Usta, M., Khan, I., Ranjan, D., & Aidun, C. K. (2022). Chemically reacting turbulent mixing in coaxial miscible liquid jets under variable viscosities and reaction rates. *SSRN Electronic Journal*.

11. Pei, B., Lai, Z., Zhao, K., Huang, N., & Bai, B. (2024). Enhancing thermal mixing of supercritical water through a confined co-flowing planar jet. *Physics of Fluids*, *36*(1), 015114.

12. Ba, Z., Wang, Y., Zhao, J., Hao, Z., Li, C., Yang, X., & Fang, Y. (2023). Comparative study on gas-particle transport characteristics subjected to the central and annular coaxial jets. *Powder Technology*, *413*, 118080.

13. Wan, Z., Yang, S., Hu, J., & Wang, H. (2023). Multiphysics coupling investigation of interphase heat transfer in gas-particle coaxial-jet swirling flow via CFD-DEM-CHT. *Chemical Engineering Journal*, *465*, 142870.

14. Wan, Z., Yang, S., Hu, J., & Wang, H. (2024). Density effect on the phase interaction mechanism of binary particle mixture in gas-particle swirling co-axial jets. *Powder Technology*, *436*, 119438.

15. Sun, H., Wang, X., Tao, X., & Li, Y. (2024). Velocity and area ratio effects on a coaxial impinging jet. *Physics of Fluids*, *36*(11), 113110.

16. Yan, S., Liu, N., Wang, B., Lv, F., Dong, X., Du, S., Yang, X., Ma, L., Yu, Q., & Bai, Z. (2024). On the effect of axial inlet angle on the droplet size distribution and mixing uniformity for swirl jet mixer at high phase ratios. *Chemical Engineering Research and Design*, *208*, 500-514.

17. Markal, B., & Aydin, O. (2018). Experimental investigation of coaxial impinging air jets. *Applied Thermal Engineering*, *141*, 1120-1130.

18. Terekhov, V. I., Kalinina, S. V., & Sharov, K. A. (2016). An experimental investigation of flow structure and heat transfer in an impinging annular jet. *International Communications in Heat and Mass Transfer*, *79*, 89-97.

19. Djeridane, T. (1994), “Contribution a` l’étude expérimentale de jets turbulents axisymétriques à densité variable”, Thèse de Doctorat, Université´ d’Aix-Marseille II, Marseille

20. Gazzah, M. H., & Belmabrouk, H. (2014). Local entropy generation in co-flowing turbulent jets with variable density. International Journal of Numerical Methods for Heat & Fluid Flow, 24(8), 1679-1695

21. Elkaroui, A., Ben Haj Ayech, S., Gazzah, M. H., Mahjoub Saïd, N., & Le Palec, G. (2018). Numerical study of local entropy generation in a heated turbulent plane jet developing in a co-flowing stream. Applied Mathematical Modelling, 62, 605-628.

22. Liu, Y., Hu, W., Zhu, R., Safaei, B., Qin, Z., & Chu, F. (2022). Dynamic responses of corrugated cylindrical shells subjected to nonlinear low-velocity impact. Aerospace Science and Technology, 121, 107321.